2001, 11, 07

The Radiation Damage Performance of Marconi CCDs

Mark Robbins

Space and Communications Group
Marconi Applied Technologies
106 Waterhouse Lane
Chelmsford Essex CM1 2QU
United Kingdom

email: mark.robbins@eev.com

Approved for distribution:

Dr Paul Jerram
Solid State Technology Product Group

1. INTRODUCTION

The radiation response of Marconi (formerly EEV) CCDs have been subject to detailed investigation over many years by several independent groups (For example Centre for Radiation Damage Studies, Brunel University, UK and Leicester University, UK) for many performance critical applications within radiation environments including European Space Agency programmes and those for high energy particle physics experiments (at the Stanford linear collider and at CERN). The following is a brief summary of our current understanding of radiation effects in Marconi CCDs and a review of some of the available results is presented. However, there is still a significant amount to do to fully understand and model all the radiation effects and suggestions for further study are made throughout the text.

2. DARK SIGNAL INCREASE

2.1. Surface generated dark signal increase in Non -IMO devices

The increase in dark signal due to ionising radiation in non-IMO devices is dominated by an increase in the generation rate of dark signal originating from the increase in the interface state density of the depleted surface areas of the device. If the substrate to gate potential is sufficiently high, holes will flood the Si/SiO_2 interface. The silicon at the surface of the channel regions becomes inverted and the Si/SiO_2 interface of the column isolation region is accumulated with holes. Therefore the dark signal from the whole of the Si/SiO_2 interface is suppressed and the only increase in dark signal with irradiation will be caused by damage to the bulk silicon which will be discussed in a later section. This suppression occurs for a substrate to gate potential around 8.5 Volts although there will be some spread around this values due to normal production spread of the buried channel implant levels. Typically the range is around 8 to 9.5 Volts. If the substrate to gate potential is reduced below this value the Si/SiO_2 interface in the channel regions depletes and charge generation starts from this area. Until the substrate to gate potential is reduced to below approximately 6 Volts (~2 volts for older devices) the Si/SiO_2 interface of the column isolation regions remains accumulated with holes and dark signal from the column isolation regions remains suppressed. In order to confine the signal within the pixel at least one phase needs to be held high. Usually this phase will be held at a gate to substrate potential of around 1.5 Volts (10 Volt clock swing). At this potential the Si/SiO_2 interface of both the channel region and the column isolation region is depleted under the high phase and thus surface dark signal from these regions is no longer suppressed.

A schematic illustration of the various contributions of dark signal for a three phase device is given in Figure 1. Here the idealised dark signal obtained by monitoring the drain current as the substrate voltage is changed, whilst connecting all the clock electrodes together at 0 Volts (static diode measurement) is compared with the idealised dark signal obtained in device operation.

The increase in dark signal has been measured for a variety of ionising radiation sources, device types and operating conditions. The radiation induced surface generated dark signal increases after irradiation has ceased (reverse annealing) and comparing various results for prediction purposes becomes difficult. However, the available results are presented here with a summary at the end of this section.

Reference [1] investigated the effects of Sr^{90} beta irradiation on Marconi CCD01 devices. These devices were used at the Stanford Linear Accelerator for the high precision vertex detector. The CCD01 was the first device type to be commercially manufactured at Marconi. The Sr^{90} beta source emits a spectrum of beta particles with an end point energy of about 2.3 MeV. The dark signal increase was measured, for device qualification, by monitoring the current in the reset drain line with the device clocking continuously (8 Volt clocks, 5 Volt substrate and 83 kHz pixel rate). Later work in Reference [2] showed that this approximates to the results obtained with the static diode measurement. The dark signal increase at 295K reported in [1], measured shortly after irradiation to 50 krad(Si) (unbiased) ranged from 5.1 nA/cm^2 (~100 pA/cm^2/krad(Si)) to 7.8 nA/cm^2 (~160 pA/cm^2/krad(Si)) over 9 devices from 5 wafer batches. Static diode measurements were made on another device at 280K. These measurements showed a linear increase with dose at a rate of 230 pA/cm^2/krad(Si) at a substrate to gate potential of 0 Volts (whole surface depleted) and 32 pA/cm^2/krad(Si) with a gate to substrate potential of 5 Volts (column isolation regions accumulated). No significant differences in the increase in dark signal were observed between irradiating the device biased and unbiased. A comparison between Co^{60} and Sr^{90} irradiation was made and showed little difference in the increase in surface generated dark signal per krad(Si).

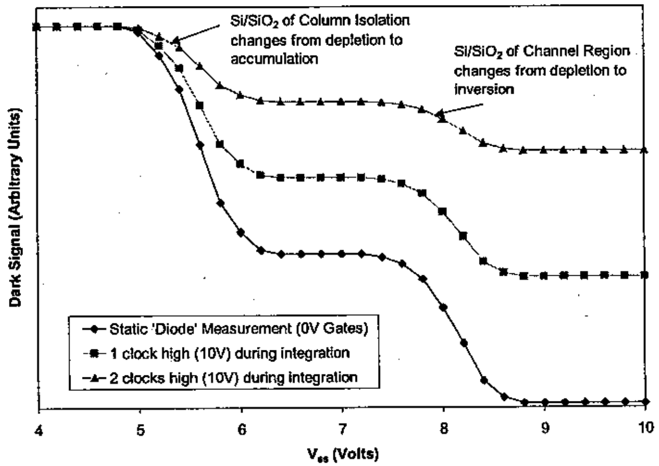

Figure 1 Simulated dark signal (clock low = 0V)

Reference [2] presented a detailed theoretical consideration of the dark signal increase in the CCD. Theoretically and experimentally it was found that the radiation induced dark signal from the Si/SiO$_2$ interface had the following temperature dependence

$$I \propto T^3 \exp\left(\frac{-7000}{T}\right)$$

Irradiations were performed using Sr^{90} betas. The surface generated dark signal increase from a CCD01 with a substrate potential of 6 Volts was measured to be 60 pA/cm^2/krad(Si) at 285K. A similar increase was obtained for a Marconi CCD02 device. Reverse annealing of the dark signal was reported. After being irradiated to 60 krad(Si) a device was left at room temperature with all connections grounded. After 18 months the dark signal at 290K, measured at a substrate to gate potential of 6 Volts, had increased by ~1 nA/cm^2. The dark signal at a substrate to gate potential of 2 Volts had increased by ~7.5 nA/cm^2.

The effect of x-ray irradiation was presented in reference [3]. Here the irradiation by a typical dental x-ray spectrum (70 kVp) was studied. Devices with and without scintillator coatings were investigated. For Co^{60} irradiations (~1.1 MeV gammas) the energy absorption coefficients for each of the different layers are similar. It is therefore straight forward to ensure that charge particle equilibrium (Compton equilibrium) exists by using build up material between the CCD and source (typically 2 mm Al). However, at x-ray energies below about 100 keV the absorption coefficient is strongly dependent on the photon energy and layer composition. The dose profiles in the dielectric layers does not approach the equilibrium values and is determined by the transport of electrons from neighbouring layers. Therefore estimating the dose actually deposited in the sensitive dielectric layers requires numerical simulation. It was found that the dose measured using a PIN photodiode was approximately 10% higher than the dose deposited in the epi layers of an uncoated CCD. The dose deposited in the gate oxide layers was calculated to be 74% that deposited in the epi. The scintillator layers can have a dose reduction or dose enhancing effect, dependent on the actual structure used. All results for x-ray irradiation refer to the dose measured by the PIN diode. The increase in surface generated dark signal at 300K for an uncoated CCD05 device, measured directly after irradiation, was 70 pA/cm^2/krad(Si) at a substrate to gate potential of 6 Volts and 200 pA/cm^2/krad(Si) at a substrate to gate potential of 0 Volts. The dark signal was measured with the device continuously clocking. The device coated with 50 µm of CsI showed a dark signal increase of 260 pA/cm^2/krad(Si) for a substrate to gate potential of 6 Volts. A device coated with 200 µm of Gd_2O_2S(Eu) showed a dark signal increase of 70 pA/cm^2/krad(Si) for the same substrate potential, similar to the uncoated case.

Reverse annealing was also studied in [3]. However, the results are not totally conclusive. A CCD05 irradiated to 10 krad(Si) showed a dark signal increase of 0.7 nA/cm^2. The device was then stored at room temperature, unbiased. The dark signal was measured at intervals over the following 7 months. After 7 months the dark signal had risen by 1.9 nA/cm^2 at 300K. However, there was no indication of the dark signal saturating. To accelerate the annealing process three devices from different batches were heated to 135 °C unbiased after being irradiated to 10 krad(Si). The reverse anneal process for one device appeared to saturate after about 600 hours. The increase in dark signal for this device was 2.5 nA/cm^2 at 280K. The increase in dark signal for the remaining two devices was about 4 nA/cm^2 after 1000 hours by which time the reverse annealing process had appeared to saturate. After 3 weeks spent at room temperature the dark signal showed a drop of 200 pA/cm^2 indicating that there is a recovery process competing with the reverse annealing process.

As in [2], the rate of increase of reverse annealed dark signal was found to be significantly higher from the depleted column isolation regions than the channel region of the devices. The reverse annealing effect was found to be significantly reduced if the column isolation is accumulated rather than depleted during the anneal. However, magnitudes are not easy to extract from the data. There is also a suggestion from the work in [3] that the final anneal dark signal is not dependent on the initial irradiation level. However the data does not clearly support this view.

The functional form of the dark signal versus temperature was not explicitly calculated in [3]. However, using the presented data, the radiation induced and reverse annealed dark signal was found to have the form

$$I \propto T^3 \exp\left(\frac{-7100 \pm 100}{T}\right)$$

Marconi CCD25 devices for the MERIS programme of the ESA Polar Orbit Earth-Observation Mission were irradiated with Co^{60} gammas and 10 MeV Protons as part of the evaluation exercise [4]. Two devices were irradiated with Co^{60} gammas up to a total dose of 26 krad(Si)[1]. All irradiations and anneals were undertaken with the device biased (clocks held low). The dark signal was measured by integrating with two phases held high (10 Volts) and with a substrate potential of 9 Volts. One device showed a dark signal increase of 1.0 pA/cm^2/krad(Si) at -25 °C. The increase seen by the second device was slightly higher at 1.2 pA/cm^2/krad(Si). A further two devices were irradiated with a combination of Co^{60} gammas and 10 MeV protons, up to a total ionising dose of 26 krad(Si) from the gammas and 7 krad(Si) from the protons. (1 krad(Si) of 10 MeV protons is equivalent to a fluence of 1.7 10^9 cm^{-2}). Extrapolating the results indicates that the 10 MeV protons caused a dark signal increase of approximately 3.5 pA/cm^2/krad(Si) at -25 °C. However, there will be a large contribution of dark signal generated from the depleted bulk silicon in this figure as discussed in a later section.

A 168 hour, 100 °C anneal was undertaken on the irradiated devices as part of the MERIS evaluation. The anneals occurred after the final irradiation step. The biasing during the anneal was as used during the Co^{60} irradiations. After this anneal the Co^{60} only irradiated devices showed an increase of approximately 300 pA/cm^2 measured at -25 °C. The Co^{60} plus proton irradiated devices gave an increase of 180 and 270 pA/cm^2.

As part of the MERIS LAT [5] three CCD25 devices were irradiated to 1.5 krad(Si) with Co^{60} gammas under the same condition as the evaluation programme. The devices were annealed at 100 °C for 168 hours and the dark signal measured. All the devices showed a dark signal increase of around 40 pA/cm^2 at -25 °C over pre irradiation levels. This increase does appear to be quite high in relation to the low level of ionising dose received. However this may confirm the observation in [3] that the increase in annealed dark signal is independent of initial radiation level, at least for low initial radiation levels.

Further work was performed on two CCD25 devices [6] to investigate the annealing performance. Two annealing temperatures were used (50°C and 100°C). Saturation of the dark signal had not been reached after 85 hours at 100°C plus 40 hours at 50°C. The results appeared to indicate that the maximum dark signal achieved by the anneal was dependent on

[1] The target total ionising dose was 20 krad(Si). It is now clear that the dosimetry carried out by Brunel University was in error. The applied doses were , in fact, 30 % higher than actually stated at the time and presented in the project evaluation reports. Both the MERIS and GOMOS programmes were affected by this error. Brunel University has produced a discussion document and an impact statement, dated 27th January 1997, as an appendix to the production screening and lot acceptance report for MERIS. The dose values presented in this report have taken into account the required correction.

the anneal temperature. Although, once again, this is not totally clear from the data.

The available data on the surface generated dark signal is summarised in the following table. Much work is required to fully understand and parameterise the increase in surface dark signal after irradiation and anneal. A carefully planned programme of work is required to establish if, and to what extent the annealed dark signal is independent of the initial radiation level. Also isochronal and isothermal anneals should be undertaken to establish the time constant of the anneal process, if it turns out that the maximum annealed dark signal is not dependent on the anneal temperature.

It must be noted that the reverse annealing of the surface dark signal observed in Marconi devices is significantly lower than that observed in CCDs manufactured using LOCOS column isolation [7].

Summary of Available Results for Dark Signal Increases in Non-MPP Devices

Measurements made directly after irradiation

Normalising T(K) 293
Normalising E/k (K) 7000

Ref	Radiation Type	CCD Type	Front/ Back Face	Coating	Clocked/ Static/ Integrated	Substrate Potential (Volts)	# Phases High During Integration	Meas Temp (T)	Min Id Increase (pA/cm² /krad(Si))	Max Id Increase (pA/cm² /krad(Si))	Scaled Min Id Increase (pA/cm² /krad(Si))	Scaled Max Id Increase (pA/cm² /krad(Si))
1	Sr90	CCD01	FI		Clocked	5		295	100	160	83.3	133.3
1	Sr90	CCD01	FI		Static	0		280	230		799.1	
1	Sr90	CCD01	FI		Static	5		280	32		111.2	
2	Sr90	CCD02	FI		Static	6		285	60		127.5	
3	70 kVp X	CCD05	FI		Clocked	6		300	70		37.3	
3	70 kVp X	CCD05	FI		Clocked	0		300	200		106.7	
3	70 kVp X	CCD05	FI	50 µm CsI	Clocked	6		300	260		138.7	
3	70 kVp X	CCD05	FI	200 µm Gx	Clocked	6		300	70		37.3	
4	Co60	CCD25	BI		Integrated	9	2	248	0.95	1.2	119.6	151.0
6	Co60	CCD25	BI		Integrated	8	2	263	9.9	22.7	208.9	479.0

Annealed Dark Signal

Ref	Radiation Type	CCD Type	Front/ Back Face	Coating	Clocked/ Static/ Integrated	Substrate Potential (Volts)	# Phases High During Integration	Meas Temp (T)	Total Dose Before Anneal (krad(Si))	Anneal Temp (T)	Anneal Time (hours)	Biased/ Unbiased	Id Increase (nA/cm²)	Scaled Id Increase (nA/cm²)	Scaled Id /dose (nA/cm² /krad(Si))
2	Sr90	CCD01	FI		Static	6		290	60	290	13000	unbiased	1	1.3	0.0
2	Sr90	CCD01	FI		Static	2		290	60	290	13000	unbiased	7.5	9.9	0.2
3	70 kVp X	CCD05	FI		Clocked	6		300	10	290	5000	unbiased	1.9	1.0	0.1
3	70 kVp X	CCD05	FI		Clocked	6		280	10	408	600	unbiased	2.5	8.7	0.9
3	70 kVp X	CCD05	FI		Clocked	6		280	10	408	1000	unbiased	4	13.9	1.4
4	Co60	CCD25	BI		Integrated	9	2	248	26	373	168	biased	0.3	37.8	1.5
5	Co60*	CCD25	BI		Integrated	9	2	248	1.5	373	168	biased	0.04	5.0	3.4
6	Co60	CCD25	BI		Integrated	8	2	263	5	85h@373K+40h@323K		biased	0.6	12.7	2.5

* dark signal increase includes prompt increase plus increase due to anneal

2.2. Surface generated dark signal in Inverted Mode devices

In Marconi IMO devices running with the silicon inverted at the silicon/silicon dioxide interface almost all of the generation of electron hole pairs from this region is suppressed. Therefore the increase in dark signal from ionising radiation is extremely small. The only absolute measurement we have at present gives a figure of 1.5 pA/cm²/krad(Si) at 30 •C. This measurement, however, was not made on the Marconi• standard• production process. However, some measurements have been made by Brunel University on standard devices. No increase was observed above their measurement resolution of 1 pA/cm²/krad(Si) at 20 •C. No reverse annealing has been reported.

When the device is being read out it is necessary to take the surface out of inversion. Thus the dark signal due to the interface states will be generated as described in the previous section. However, the dark signal due to interface states collected during readout will be significantly suppressed by the effect of dither clocking.

2.3. Bulk Dark Signal

If the incident radiation has sufficient energy to displace a silicon atom from its lattice position defect states within the silicon band gap will be formed. If these are situated within the depletion region of the device they will act as dark signal generation centres.

2.3.1. Mean Level

Based on theoretical considerations, it was shown in [2] that the bulk generated dark signal should be proportional to the depletion volume. For a mid gap generating centre in the bulk silicon, the theoretical variation of dark signal with temperature was given as

$$I \propto T^2 \exp\left(\frac{-7000}{T}\right)$$

Note that the pre-exponential term is now T^2 compared with T^3 as in the case of surface generation. Bulk dark signal increase by Sr^{90} beta radiation[2] was measured to give a temperature dependence of

$$I \propto T^2 \exp\left(\frac{-6405}{T}\right)$$

The lower activation energy could not be explained theoretically as a dominant defect away from mid gap would cause a higher activation energy. The discrepancy was put down to experimental error in the determination of the leakage currents and the low levels of dark signal actually being measured.

Detailed work on Cf^{252} neutron irradiated devices [8] showed quite clearly that the bulk dark signal was proportional to the depletion depth. The work gave a figure at 305K of

$$I = 3.5 \times 10^{-8} \phi$$

where I is the dark current per unit depletion volume (nA/cm³) and ϕ is the 1 MeV equivalent

[2] The endpoint of the Sr^{90} beta spectra is 2.3 MeV whereas electron energy of only around 210 keV is required to displace a silicon atom

neutron fluence (cm^{-2}). This figure was the same for high (1500 Ocm) and low (20 Ocm) resistivity material.

Work performed on proton irradiated CCD02s in [8] estimated that at 300K after 3.6 10^9 10 MeV equivalent p/cm^2 the bulk dark signal increase was 0.25 nA/cm^2 on low resistivity material and 1.25 nA/cm^2 on high resistivity material; the difference being due to the difference in the depletion depth.

Work performed on CCD02s for the ESA SILEX programme is reported in [9]. Here 10 MeV protons were used to investigate bulk and surface damage. After 1.6 10^{10} cm^{-2} of 10 MeV protons the dark signal had increased by approximately 2 nA/cm^2 at 292 K. However, this did include the surface component of dark signal. It was noted that the bulk damage was independent of the device's bias state during the irradiation. From the dark signal distribution it was found that significant annealing of the bulk dark signal occurs following the irradiation. Measurements taken 75 days after the irradiation showed a drop in bulk dark signal of roughly 50% compared with data taken 12 days after irradiation. The devices had been stored at room temperature. Further work is required to determine the activation energy and thus the time constant for this annealing process.

It has been established that the mean level of bulk dark signal scales approximately with the mean non ionising energy lost (NIEL) to the silicon by the incident radiation [10]. Detailed work performed on Marconi CCD47 devices [11] looking at dark signal degradation caused by 60 MeV protons has established the following useful relationship

$$\Delta s \approx 10^{-5} \times V \times \phi \times NIEL \times T^2 \exp\left(\frac{-6616}{T}\right)$$

where ?s is the mean dark signal increase in electrons per pixel per second measured 3 months after the irradiation, V is the depletion volume of the pixel in μm^3, F is the proton fluence in cm^{-2} and NIEL is the non ionising energy loss measured in keVcm^2/g. The temperature dependence was measured over a limited temperature range of 274K to 298K. The dark signal distribution measured on CCD25 devices at 248 K could be accurately modelled using this relationship if the temperature was assumed to be 251 K. This slight discrepancy can be explained by the annealing behaviour as the measurements on the CCD25 device were made shortly after the irradiation.

It must be noted that, although the equation is useful for engineering purposes care must be taken when extrapolating to very high or low energies. For example, at low proton energies the NIEL may not be constant along the track through the CCD and the protons may even stop within the depletion region. This must be taken into account when estimating the mean NIEL. Also the relationship assumes that the defects dominating the dark signal generation are the same no matter what the energy of incident protons. This certainly appears true up to the 60 MeV protons tested here but it may be that at higher energies different defects are produced yielding a different scaling factor. In fact there have been some reports that the mean dark signal does not scale with NIEL at energies above 150 MeV.

2.3.2. Dark Signal Non-Uniformity (DSNU)

The dark signal non-uniformity is dominated by the bulk component of the dark signal. As described in the previous section the amount of bulk dark signal is related to the level of lattice damage. There will be stochastic fluctuations in the amount of damage produced from

pixel to pixel, causing a variation of dark signal across the CCD array. A measure of this variation is the dark signal non-uniformity (DSNU) which is often defined as the standard deviation of the distribution of dark signal generation rates of each pixel of the device. From a knowledge of the distribution of energies imparted to the silicon lattice, and the size of the depletion volume, it is possible to model the dark signal distribution [11]. A comparison of a measured and modelled distribution for a proton irradiated CCD47 is given in Figure 2.

The distribution is dependent on the nature and energy of the incident radiation, the radiation fluence and the depletion volume of each pixel. In order to estimate the dark signal distribution resulting from the damage due to a spectrum of protons it is necessary to estimate the distribution at each energy and convolve the results. The modelling is only valid if the range of recoil atoms is significantly shorter than the dimensions of the pixel depletion volume. Therefore, depending on the CCD structure, the modelling cannot be relied upon at energies greater than about 100 MeV.

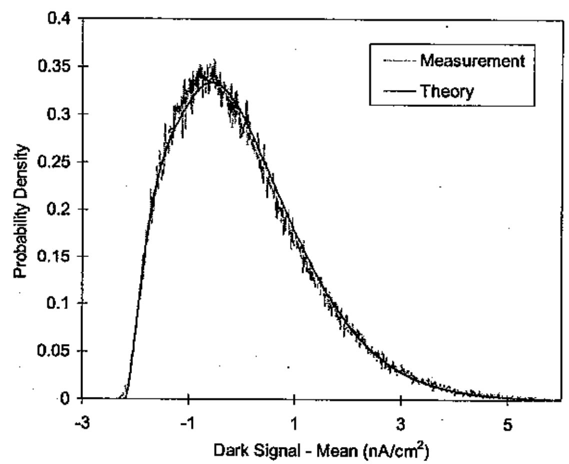

Figure 2 Dark signal distribution at 298K from a CCD47-20 after 3.4 10^{10} 60 MeV p/cm^2

2.4. Defective Pixels

It was seen in the previous section that the interaction of the protons with the silicon causes a pixel to pixel variation in the dark signal generation rate. This distribution has a significant tail simply due to the stochastic nature of the interaction. Therefore some pixels will have a dark signal generation rate significantly greater than the mean.

However, if a charge generation centre is created in a high field region of a device the generation rate from this defect will be enhanced by the lowering of the potential barrier (Poole-Frenkel effect) or by phonon assisted tunnelling. Therefore very bright pixels will be observed with a generation rate significantly outside the distribution predicted in the previous section. The Figure 3 and Figure 4 show the enhancement expected if the generation centre

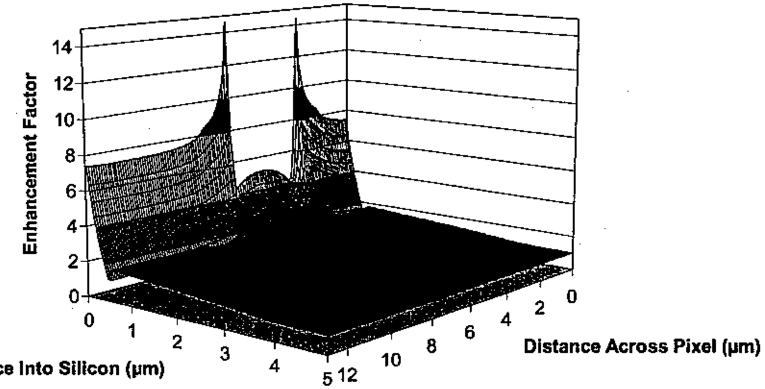

Figure 3 Field enhanced emission from Coulombic defects in CCD47-20 (2d across electrodes, 3d Pool-Frenkel)

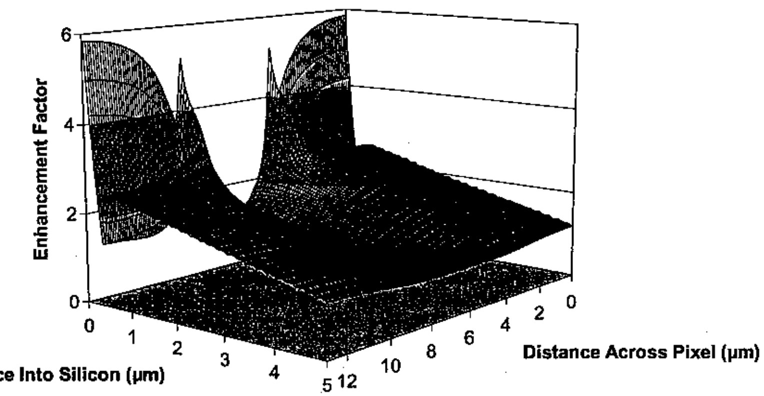

Figure 4 Field enhanced emission from Coulombic defects in CCD47-20 (2d across column isolation, 3d Pool-Frenkel)

has a coulombic potential profile. It can be seen here that the greatest enhancement occurs in the region between a gate being held high and a gate held low. The relevant volume is actually quite small so the probability of a defect being created here is low. However if a coulombic defect is created here its generation rate will be enhanced by a factor 14. This is probably over pessimistic as most deep levels are expected to be non-coulombic. Other potentials, such as the Yukawa potential, have been shown to produce a significantly lower enhancement factor [12].

Unfortunately there has not been significant work performed on the creation of defective pixels in Marconi devices. However, this was briefly investigated for Marconi CCD25 devices by SIRA on behalf of ESA[13]. It was found that after 2 krad(Si) of 10 MeV protons (equivalent to 3.6×10^9 cm^{-2} 10 MeV protons) 0.1% of the pixels had a dark signal greater than 3 nA/cm^2 at 20°C. After 4 krad(Si) (equivalent to 7.2×10^9 cm^{-2} 10 MeV protons) 0.1% of the pixels had a dark signal greater than 4.5 nA/cm^2. Some of the dark signal 'spikes' had a lower activation energy than the mean dark signal. The trend was for the largest 'spikes' to have the lowest activation energy. The activation energy of the spikes ranged from 0.37 eV to 0.68 eV.

2.5. Random Telegraph Signals

It has been observed that after proton irradiation some pixels show a temporal fluctuation in the dark signal generation rate. This fluctuation is known as a Random Telegraph Signal (RTS). RTS behaviour was studied for Marconi and Thomson devices in [14] and should be observed in all CCDs. It is characterised by sharp transitions between two or more discrete generation rates. The times spent in the high or low dark signal states are randomly distributed but the average times in each state are well defined. The time constant for each state of the RTS defect was found to have the form

$$\frac{1}{\tau} = R \cdot \exp\left(\frac{-E}{kT}\right)$$

where R ranged from 10^{13} to 10^{14} s^{-1} and E was found to be 0.9 ± 0.1 eV. This large activation energy implies that the range of temperatures for which RTS behaviour can be observed is limited. For example, at –30 °C, it was predicted that the time constants would be in the order of 6 days and at 50 °C they would be approximately 10 seconds. It was found that, although proton induced dark signal spikes were often seen to exhibit RTS behaviour, fluctuations were also often seen in 'average' pixels. The temporal fluctuations appeared to be a component additional to the background dark signal.

The RTS amplitude was found to be in the order of 0.1 nA/cm^2 at 20 °C with a temperature dependence given by exp(-(0.57 ± 0.03 eV)/kT). Measurements made on an Marconi CCD05-20 device (770 x 576 image area pixels) confirmed that the probability that a pixel contains n RTS defects follows a discrete Poisson distribution given by

$$p(n,\lambda) = \frac{\lambda^n \exp(-\lambda)}{n!}$$

where ? is the mean number of RTS defects in a pixel. It was found that, for the CCD05 device irradiated with 10 MeV protons, ? is given by

$$\lambda = 0.000013 \times A \times \phi$$

Where ϕ is the proton fluence and A is the pixel area (22.5 µm x 22.5 µm). The results are presented in Figure 5. It can be seen from these results that after 10^9 cm^{-2} 10 MeV protons it can be expected that around 27000 pixels (6% of total) may contain a single RTS type defect.

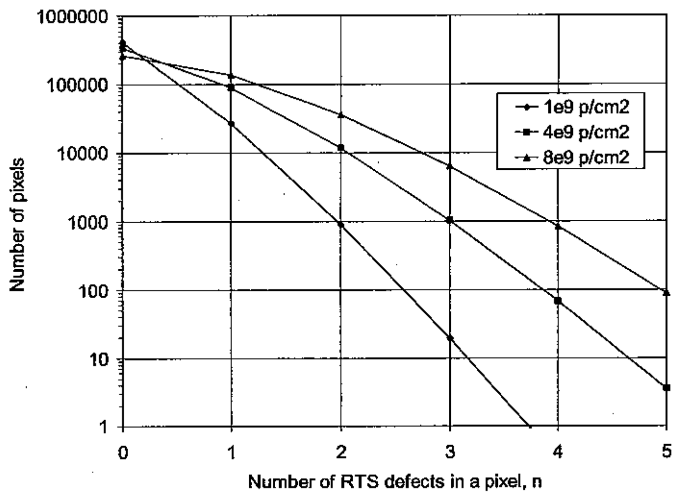

Figure 5 Number of pixels containing n RTS defects (CCD05-20) for various 10 MeV proton fluences

It was found that the RTS defect anneals out at approximately 100 °C. The mean time in the high dark signal state became progressively longer until the dark signal was permanently high.

Detailed measurements were not made at other proton energies. However some measurements were made after irradiation with 1.5 and 100 MeV protons and the indications were that the values for ? were comparable to the 10 MeV results within a factor 2 or 3. However, further work on the energy dependence of ? was undertaken in [13] and it was shown that ? scaled with the elastic NIEL and not the inelastic NIEL implying that RTS defects are not the result of nuclear interactions.

For 1.5 MeV protons it was found that

$$\lambda = 0.000125 \times A \times \phi$$

and for 46 MeV protons

$$\lambda \approx 0.000005 \times A \times \phi$$

2.6. Dither Clocking

In non IMO (non MPP) devices the surface of the silicon is depleted under at least one phase (the phase held high) and a high generation rate from the interface states results. If this phase is taken low the surface inverts with the accumulation of holes and the dark signal generation from the interface states is suppressed, leaving the much lower bulk component. If the bias is now taken back to the case that allows surface depletion, even after only a short period of inversion, the recovery of the original dark signal generation rate is not immediate. The principle of dither clocking is therefore to operate with a substrate bias high enough to invert the surface under the electrodes at clock low level and to periodically switch the clock high level electrode between the phases of each element [15,16]. Dither clocking can be used to reduce the radiation induced dark signal in non-IMO devices. The effectiveness of the dither clocking is dependent on the temperature and the dither period. Dither clocking is only effective at reducing the surface component of dark signal. It has no effect on the bulk contribution which may be the dominant source of dark signal in a proton environment.

Dither clocking was investigated as part of the MERIS program. Here the dither period was 0.77 ms and the temperature was -25 •C. The dithered dark signal was assessed after the devices had received a combination of Co^{60} gamma and 10 MeV proton irradiation and an annealing step. Dithering reduced the dark signal by approximately a factor 4. It can be expected that by optimising the biases and dither period the dark signal will be reduced even further.

Dither clocking will create defects in the image. These defects are black-white pairs with an amplitude dependent on the signal size and the number of dither periods before the image is read out. The number of defects is dependent on the dither scheme employed [16]. The number of black-white pairs for a given proton fluence appears to depend on the CCD [13]. For 1 krad (1.79 10^9 cm^{-2} 10 MeV protons) a CCD02 device gave roughly 1 in 20 pixels affected, whereas for the CCD25-20s tested the number was approximately 1 in 200. The number of pixels affected appeared to scale with proton fluence.

3. FLAT BAND VOLTAGE SHIFTS

As is common with all MOS devices, and therefore all MOS CCDs, ionising radiation causes electron hole pairs to be generated within the gate dielectric structures. The electrons and holes can either recombine or leave the dielectric without causing any net effect, or the electrons alone can leave the structure whilst leaving some of the holes trapped within the dielectric. This results in a net positive charge and a shift in the flat band voltage of the MOS structures i.e. the device behaves as if the bias applied to the gate structures of the device has increased by the amount of the voltage shift.

The number of electron hole pairs that escape initial recombination is dependant on the temperature, the density of the generated electron-hole 'cloud' and the local electric field. The temperature dependence is not a significant issue at temperatures above about 120K or so. The density of the generated electron hole pairs is dependent on the rate of irradiation and the nature of the radiation. The electron - hole density obtained from an interacting low energy x-ray is higher, for example, than an interacting 1 MeV gamma ray and so, as the initial recombination is lower, the voltage shifts obtained per unit dose is higher for Co^{60} irradiated samples. The presence of an electric field tends to separate the electron-hole pairs before they can recombine and the direction of the electric field determines where the holes will be trapped within the dielectric. The voltage shifts are also dependent on the structure of the gate dielectrics and on the processing applied. The structure of CCDs is such that if the CCD is irradiated under bias the voltage shift will be greater than if it were irradiated with all pins grounded.

3.1. Magnitude of the Shift

In [1] the voltage shift was measured on CCD01 devices unbiased and also clocking during irradiation by betas from Sr^{90}. With the device unbiased the measured voltage shift was 250 mV after 10 krad(Si) then increased approximately linearly up to 50 krad(Si) at a rate of 14 mV/krad(Si). With the device clocking at 180K the voltage shift increased linearly at a rate of 120 mV/krad(Si). This figure reduced by ~3% on warming to room temperature and a further 3% after being baked at 430K for 2 hours in a nitrogen atmosphere. 9 devices across 5 batches were assessed with devices irradiated unbiased to 50 krad(Si). All showed voltage shifts consistent to within approximately 10%.

Measurements on the voltage shift as a function of electric field in the gate dielectric of CCD01s were presented in [2]. For irradiation with Sr^{90} betas under normal operating conditions at room temperature a shift of 90 mV/krad(Si) was observed.

Measurements made after irradiation with a typical dental x-ray spectra (70 kVp) are presented in [3]. As described in Section 2 the results from low energy x-ray irradiations are complicated by dose enhancement effects so care must be taken when comparing these results with those from other irradiations presented here. However, it was observed that for uncoated CCD02s and CCD05s the measured voltage shifts were 40-50 mV/krad(Si) (devices biased during irradiation). Devices coated with CsI or Gd_2O_2S(Eu) showed a shift of 90-100 mV/krad(Si). Annealing at 408K was found to reduce the voltage shift by about 40% after 500 hours.

As part of the MERIS evaluation exercise [4], voltage shifts were measured after Co^{60} irradiation by noting the shift in the substrate potential at which the surface becomes pinned. The devices were irradiated biased with Co^{60} gammas. The measured shift was (80±15) mV/krad(Si), the uncertainty coming from the uncertainty in the dosimetry and the

measurement.

As part of the formal GOMOS (CCD26, back illuminated) evaluation exercise [17] irradiations were also performed with Co^{60} gammas. The voltage shift was estimated from the gate capacitance versus substrate potential plots. The result was a voltage shift of 100 ±20 mV/krad(Si).

There has not been significant work undertaken on the voltage shifts caused by protons with the devices under bias. The work that has been undertaken confirms the work undertaken on MOS transistors [18,19] that indicates that the voltage shift caused by a rad(Si) of protons having energy greater than about 10 MeV is about the same as that measured with Co^{60} gammas. However, as the energy is reduced below 10 MeV there is increasingly greater initial recombination of the electron hole pairs and the voltage shifts per rad(Si) tend to be lower.

3.2. Effect of the Voltage Shifts on Device Performance

Irradiation changes the operating point of the CCD as if the biases applied to the gates of the device have been offset by an amount equal to the flat band voltage shift. If no correction to the bias supplies can be made then a realistic maximum voltage shift that can be accommodated whilst still maintaining device performance is approximately 2 Volts as illustrated in this section.

As the CCD is irradiated the channel potential for a given gate potential increases. The main implication of this is that the charge storage capacity of the output node reduces with increasing voltage shift. The output node storage capacity will be reduced roughly linearly with ionising dose. This is illustrated in Figure 6.

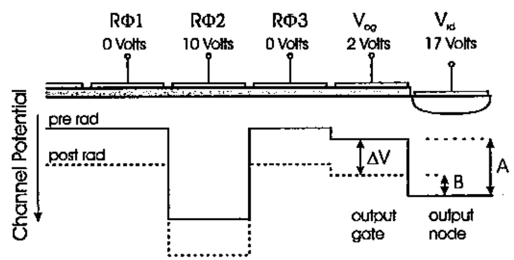

Figure 6 A schematic of the channel potential around the output node. A and B represent the node storage capacities before and after irradiation.

As the device is irradiated the substrate to gate potential at which the surface inverts increases by the amount of the voltage shift. Therefore, there comes a point at which an abrupt increase in dark signal is observed as the surface comes out of inversion. The device can be set up before irradiation such that an ~2 Volt shift (~20 krad(Si)) can be accommodated before this occurs. The transition from 'low' to 'high' dark signal will not be a sharp step but will occur over a shift of about 1 Volt (~10 krad(Si)). During this transition phase the DSNU will be high due to different areas of the silicon/silicon dioxide interface coming out of inversion at slightly different points.

Prior to irradiation, the Reset FET will turn off at a gate voltage around 4 Volts (gate to source voltage of −13 Volts). After a voltage shift of approximately 4 Volts the reset FET will no longer be able to turn off using the usual 0 to 10 Volts reset clock. This results in a severely smeared picture and failure of the device. The responsivity (Gain) of the amplifier will have also dropped by this time as the amplifier FETs are no longer biased at the optimum point within their characteristics. The responsivity drop is dependent on the type of output circuit (one or two stage) and how the output amplifier is set up prior to irradiation. The responsivity change measured for the single stage amplifier of the CCD25 after Co^{60} irradiation is shown in Figure 7. The biases were optimised for device amplifier linearity and were satisfactory for the mission dose range of around 2 krad(Si). The drop in gain at higher doses could have been reduced by selecting different bias conditions prior to irradiation. This optimisation will be discussed in the following section. It may be expected that the gain change for a two stage amplifier will be greater. However, this has not been assessed in detail.

As well as these 'major' changes observed with increasing voltage shift, there will be other changes. For example, the full well capacity of the array may increase due to an increase in effective clocking potentials. The change in the operating point of the output circuit will cause a change (decrease) in DC power consumption and also a change in the output waveform features. A general decrease in the total leakage current has also been observed.

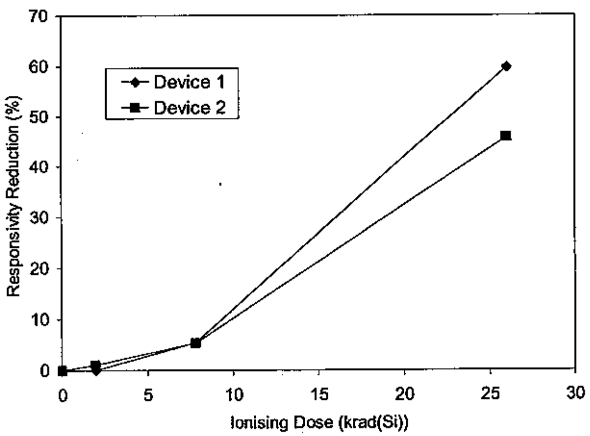

Figure 7 The change in responsivity of CCD25 biased during irradiation

3.3. Bias set up for optimum radiation performance

In order to obtain the maximum radiation performance from the device, biases must be chosen to take into account the radiation induced voltage shifts. The biases are dependent on the level of voltage shift that must be accommodated and also the buried channel implant levels which will vary from device to device through normal production spread. The optimum

biases will thus be device dependent. The biases must be set such that at the end of life the surface still inverts at image clock low level, the output node capacity remains sufficient and the output FETs continue to operate in the optimum region of their characteristics. When choosing the biases it is important to ensure that the surface under the output gate is not be pinned to ensure good transfer of charge to the output node at the start of life. In addition the pulses applied to the reset FET must be considered, taking into account the inevitably high level of V_{rd}. A suggested method for choosing the correct biases for a particular device is as follows:

i) Note the substrate to gate pinning potential, V_{ssp} from an I_{rd} versus substrate potential curve or from the results of the parametric tests performed on test structures. The pinning potential will normally lie within the range 7.5 to 9.5 Volts. Assuming the image clock low level is at 0 Volts, choose a substrate potential of ?+Vssp, where ? is the voltage shift to be accommodated (including margin).

ii) Next, the output gate potential, V_{og}, needs to be set. As the Si/SiO_2 interface must not be pinned, V_{og} must be chosen such that the substrate potential (V_{ss}) minus V_{og} < V_{ssp}- 1 Volt. If V_{ss} is chosen as in i) this leads us to choose V_{og}> ? + 1. As a minimum. V_{og} is usually chosen to be 3 volts.

iii) The choice of reset drain potential, V_{rd}, is dependent on the node capacity required at the end of life, V_{node}. To a first approximation the maximum potential swing at the node is given by V_{rd} minus the channel potential under the output gate which is approximately given by V_{og}+ f $_{ch0}$ where f $_{ch0}$ is usually in the range 10 to 13 volts. It must be noted that other second order effects should be considered for detailed analysis but this approximation will serve for illustration purposes.

Following a voltage shift of ? the channel potential under the output gate becomes approximately V_{og} + f $_{ch0}$ + ? . Therefore to accommodate an end of life V_{node}, V_{rd} should be set to

$$V_{rd} = V_{node} + V_{og} + f_{ch0} + ? + a$$

a takes into account the drop in node potential due to charge partition in the reset FET on turning the reset FET off (reset feet through) ~ 0.5 Volts.

iii) To ensure the buried channel output circuit source follower FETs remain operating optimally at end of life it is necessary to ensure that the output drain potential is set to

$$V_{OD} = V_{rd} + f_{ch0} + ?.$$

v) The reset pulse high level must be sufficient to turn on the reset FET. The reset FET will turn on at a gate potential approximately equal to V_{rd} - f $_{ch0}$.

To ensure a channel of sufficient conductance is formed a margin of roughly 1 Volt is required. Therefore, as a minimum the reset high level should be set to

V_{rd} - f $_{ch0}$+ 1.

vi) The reset pulse low level must be sufficiently low so that the reset FET does not 'turn on' when the maximum charge appears at the node. Therefore the reset FET low level must be below V_{rd} - f $_{ch0}$ - V_{node} - 1.

vii) For AIMO (MPP) devices the image/store clock high level must be sufficient to transfer signal. This level is dependent on the buried channel implant, the IMO implant and the substrate potential. The higher the substrate potential is set to, the higher the required clock high level. A clock high level of greater than 15 Volts may be required. However, high clock and substrate potentials will increase the risk of charge generated through impact ionisation. This will lead to a low level of excess signal which is only important in situations requiring the minimum noise and dark signal, eg. X-ray spectroscopic applications. For normal imaging applications this should not be significant.

As an example of setting the biases, a f_{ch0} of 11 V and a V_{ssp} of 8.5 V is assumed. The required ? is assumed to be 1 Volt and the required end of life node capacity of 3 Volts. Using the approximate relationships above we obtain the following

Substrate potential should be set to 9.5 Volts

Output gate set to 3 Volts

Reset drain set to 18.5 Volts

Output drain set to 30.5 Volts

Reset FET high level > 8.5 Volts

Reset FET low level < 3.5 Volts

A slightly more detailed analysis of the channel potential under the output gate, by solving the Poisson equation assuming stepped doping profile, gives the following

Substrate potential should be set to 9.5 Volts

Output gate set to 3 Volts

Reset drain set to 19 Volts

Output drain set to 31 Volts

Reset FET high level > 9 Volts

Reset FET low level < 4 Volts

3.4. Tracking the voltage shift

There are some practical limitations to the extent at which the CCD biases can be set to accommodate the voltage shifts experienced through life. For example, some devices may cease to operate satisfactorily at a substrate potential greater than ~11 Volts prior to irradiation and too high an output drain potential will lead to excess noise which may be unacceptable in some situations. The practical limit for setting the biases as in the previous section is to accommodate around a 1.5 to 2 Volt shift. This occurs at an ionising dose from Co^{60} gammas of 15 to 20 krad(Si). The devices will operate up to higher dose levels but the performance will be severely degraded.

If some form of bias tracking can be employed the voltage shift that can be accommodated will be much greater (between roughly 3 or 4 Volts). As the device is irradiated the low and

high clock levels will have to be reduced, the output gate, dump gate and anti-blooming gate bias reduced and the output drain voltage increased, all by the amount of the voltage shift. Alternatively the clock levels can be kept fixed with the drain and substrate biases increased. The output drain bias should be increased at twice the rate to preserve the gain. If the CCD has a dummy output FET and is not being used to cancel common mode noise, it is conceivable that it can be used to monitor the voltage shift and to feed back to some compensation circuitry. Marconi, however, has not developed such a system.

3.5. Radiation tolerant technology

Marconi have supplied devices for TV rate applications that experience a significantly reduced voltage shift. These device remain operational at ionising doses greater than 1 Mrad(Si). The process can theoretically be applied to any device type although evaluation of the process would be required for performance critical applications.

4. CHARGE TRANSFER DEGRADATION

4.1. Introduction to CTE degradation

The charge transfer efficiency (CTE) is defined as the fraction of the signal when transferred from one pixel to the next. The charge transfer inefficiency (CTI) is defined as 1 - CTE. The observed image degradation due to a loss of CTE is a strong function of the operating conditions of the CCD and the type of image being observed. It is not possible to quote a single figure for the CTE degradation that covers all operating conditions, image types and CCD structures. Measured CTE figures are only directly relevant to the device type under test, running under the test operating conditions and with the images used for the test measurement. Therefore, to estimate the degradation that will be observed in practice it is necessary to understand the theory behind charge trapping and how the distributed signal within the CCD interacts with the traps. The theories are covered in detail within the quoted references. However, the main elements are presented here to illustrate the type of degradation to be expected. Because the CTE is so dependent on the measurement conditions, only results directly relevant to the predictions are presented here. It was noted in [20] that it is probably not possible to predict effects to better than a factor two to three from published data because of variations in the operating conditions and the measurement techniques used in a given laboratory. For these reasons it was recommended that, for critical space applications, ground testing tailored to reflect the in-orbit conditions as close as possible be carried out.

4.2. Main defects responsible

If a semiconductor material is placed in a radiation environment having sufficient energy to displace atoms from there lattice positions, discrete energy levels will appear within the band gap. The vacancies produced by the radiation are dispersed through the lattice and combine with available atoms or other vacancies. The exact combination determines the nature of the energy levels. For example, in silicon, a vacancy teaming up with a phosphorus atom creates the P-V centre (Si-E centre) having an energy level around 0.44 eV below the conduction band edge and an electron capture cross section around 2 10^{-15} cm^2. This is usually the dominant radiation induced defect that is responsible for the CTE degradation in CCDs. There are other defects produced such as the oxygen vacancy complex (Si-A) centre and the divacancy (V-V). Divacancy production is not significant in electron irradiated devices but is important in proton irradiated devices. Despite this complication, it has been found that the CTE degradation scales with NIEL, independent of particle type and energy, at least to a first approximation.

Work performed in [1] on high energy electron irradiated Marconi CCD01s measured the introduction rate of the Si-E centre to be

$$N_t\,(cm^{-3}) = (2.0 \pm 0.6) \times NIEL\,(keVcm^{-2}/g) \times F\,\,(cm^{-2})$$

where F is the particle fluence.

The number of defects produced by proton irradiation is dominated by the Si-E centre. However, the divacancy is also important. Work published in [21] on 10 MeV proton irradiated devices (not Marconi CCDs) showed an introduction rate of the Si-E centre as

$$N_t\,(cm^{-3}) = 2.5 \times NIEL\,(keVcm^{-2}/g) \times F\,\,(cm^{-2})$$

And for the divacancy

$$N_t\,(cm^{-3}) = 0.4 \times NIEL\,(keVcm^{-2}/g) \times F\,\,(cm^{-2})$$

The divacancy creates two electron traps, one at an energy level within the silicon band gap similar to the Si-E centre, the other much shallower at around 0.21 eV below the conduction band edge.

4.3. Theory of charge trapping

The basic theory of charge trapping has been discussed by many authors and will be covered here to illustrate the main points of CTE degradation. Only trapping from traps with a single energy level will be covered but the theory can easily be extended to multiple trap types.

Since the signal is transferred in the depletion region, the only important mechanisms are capture of signal electrons from the conduction band and their subsequent emission back to the conduction band from the trapping centre. The time constants for the capture (t_c) and emission (t_e) processes are

$$\tau_c = 1/(\sigma_n v_{th} n_s)$$

$$\tau_e = \exp(E/kT)/(\sigma_n X_n v_{th} N_c \chi)$$

Where

n_s	=	signal density
s_n	=	electron capture cross section
v_{th}	=	mean thermal velocity for electrons
N_c	=	effective density of states in the conduction band
T	=	Temperature
k	=	Boltzmann's constant
X_n	=	'entropy factor'
χ	=	field enhancement factor
E	=	energy level of the trap below the conduction band edge

The field enhancement factor was added in [22] to allow for possible increased emission rates in high field regions of the device. In practice χ was found to be very close to unity.

First we will consider the emission of charge from the traps. When a charge packet is present in a pixel s_t electrons will be trapped within the pixel volume. If the charge packet is transferred from this pixels, and no other charge packet follows, then s_t decreases exponentially so that

$$\frac{ds_t}{dt} = -\frac{s_t}{\tau_e}$$

i.e.

$$s_t = s_{t0}\exp(-t/\tau_e)$$

If another charge packet, the same size as the first, is transferred to the pixel, the number of electrons trapped and lost from this charge packet will now be

$$s_{lost} = s_{t0}(1 - \exp(-t_0/\tau_e))$$

where t_0 is the time between charge packets passing through the same pixel. Thus, if the time between charge packets is very much less than the emission time constant of the trap, the traps would not have emitted the charge captured from the previous charge packet and therefore do not contribute to the reduction in the apparent CTE.

The emission time constant is a sensitive function of the energy level of the trap. The range of published data on the trap energy levels and capture cross sections for a particular defect varies enough for there to be significant uncertainty in the emission time constant if it were calculated using published data. Probably the most reliable data, suitable for use in our calculations, is that obtained using the CCD itself to calculate the emission time constant. The emission time constant of the dominant defect (Si-E centre) published in [22] was measured using a proton irradiated CCD02. The published results are as follows

Temp (K)	293	280	268	253
t_e (μs)	22	64.5	120	430

This data is consistent with an energy level below the conduction band edge of 0.42 ± 0.03 eV and a capture cross section in the order of 10^{-15} cm^2.

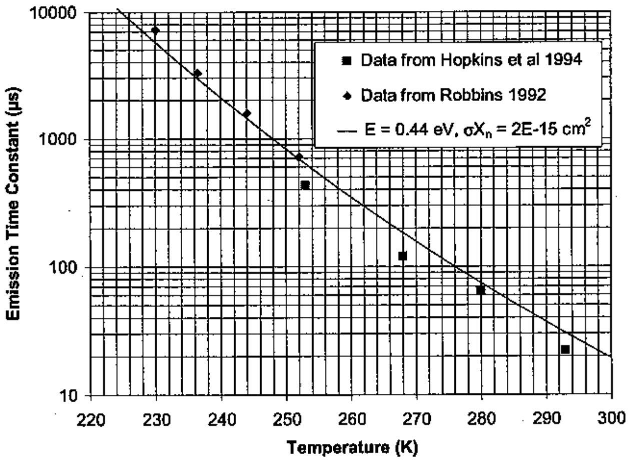

Figure 8 The published values of the emission time constant of the Si-E centre measured using the CCD. The line is calculated assuming a trap energy level of 0.44 eV and a cross section multiplied by the entropy factor of 2 10^{-15} cm^2.

The energy level and capture cross section of the Si-E centre was measured in [1] using electron irradiated CCD01 devices. Here the energy level was measured to be 0.47 ± 0.03

eV and a capture cross section of (3 ± 1) 10^{-15} cm^2, assuming an entropy factor of 1.7.

The emission time constant, for the Si-E centre, as a function of temperature is plotted in Figure 8. Figure 9 shows how the time between charge packets affects the amount of charge trapped from the signal. The plot can be thought of a normalised CTI (CTI = 1-CTE), normalised to the maximum CTI. As the time between bursts of signal decreases, less time is available for the traps to emit their charge. Therefore the low temperature side of the peak shifts towards higher temperatures where the emission time constant is reduced. In x-ray spectroscopic applications, for example, the data is very sparse, i.e. t_0 can be quite long. Therefore, to minimise the CTE degradation and thus optimise the spectroscopic resolution, the CCD must be cooled so the traps remain filled for long periods of time. It is not unusual, in these situations, to run the CCD at temperatures around 180K. Work performed in [8] studied the effect of x-ray hit rate in detail for the XMM mission.

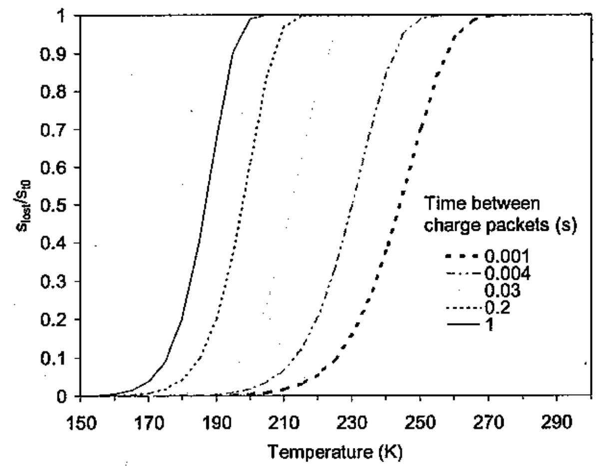

Figure 9 Calculated s_{lost}/s_{t0} for various times between charge packets.

If the emission time constant is very much shorter than the clock period then the electrons, if trapped, can be re-emitted back into the signal, thus reducing the CTI. This is illustrated in Figure 10 which shows the result of modelling the shallower divacancy level (E = E_c – 0.21 eV s_n = 5 10^{-16} eV ref [21]) assuming a clocking frequency of 10 kHz and a time between charge packets of 1 second. In this situation this trap has little effect on the CTE above about 180K.

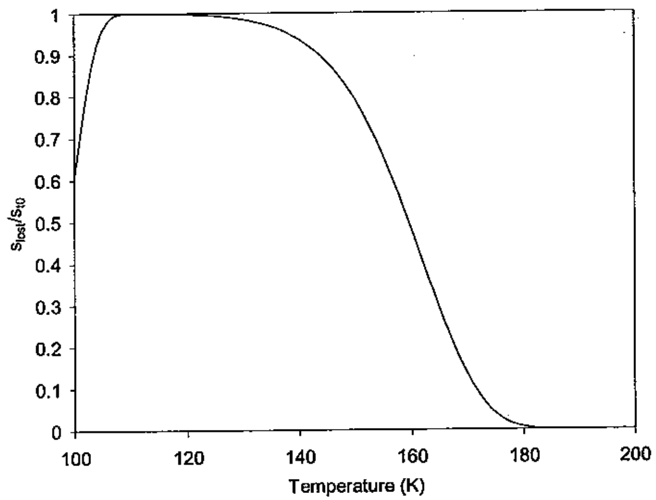

Figure 10 Modelling of the effect of the shallower divacancy trap for a clocking frequency of 10 kHz.

4.4. The signal density

If charge is transferred to a gate having empty bulk traps, the traps will fill so that, after a time t_g, the density of filled traps will be

$$n_t = \frac{N_t \tau_e}{\tau_c + \tau_e}\left(1 - \exp\left(-t_g\left(1/\tau_c + 1/\tau_e\right)\right)\right)$$

where N_t is the trap density. If $t_e >> t_c$ then this simplifies to

$$n_t = N_t\left(1 - \exp\left(-\frac{t_g}{\tau_c}\right)\right).$$

It is straight forward to calculate n_t if the signal density, and thus t_c, is constant over the signal volume. Unfortunately, this is not the case, as discussed in the following paragraphs. However, in the simple case of zero background signal an effective signal density, n_s, may be defined. In this case the CTI can then given by

$$CTI = \frac{N_t}{n_s}\sum_{i=1}^{3}\left(1 - \exp\left(-\frac{t_{gi}}{\tau_c}\right)\right)$$

where the sum is over the 3 gates that make up a pixel in a three phase CCD. If the time spent under a gate is < the capture time constant not all the traps will be filled by the time the signal is transferred to the next phase. Therefore the CTI will be reduced from its maximum value. Thus high speed clocking may be desirable in some situations.

n_s is a strong function of signal size, increasing with increasing number of electrons in the signal. Thus the CTI can be considerably higher for small signals than observed with larger signals. For example, the effective signal density for the readout register of a CCD01 (register pixel size = 22 µm x 88 µm) was measured to be 3 10^{13} cm^{-3} for a signal size of 500 electrons, increasing to about 2.5 10^{14} cm^{-3} for a signal size of 70,000 electrons (ref [1]).

By confining the signal to smaller volumes the effective signal density increases. This has the effect of reducing the number of traps the charge packet 'sees'. This is the principle behind the use of a supplementary buried channel (notch) which can be effective in reducing the CTE degradation for small signals. However, increasing the effective signal density reduces the capture time constant which may adversely affect the CTI, dependent on the clocking frequencies used.

When estimating the CTI with a background signal it is necessary to look at the charge distribution in detail. Simulations have been undertaken by Marconi Applied Technologies and the results for the charge distribution for two different signal levels are shown in the following plots. The simulation here has been done on a CCD02 structure (22 µm x 22 µm pixel) assuming a stepped buried channel doping profile (N_d = 2.5 10^{16} cm^{-3} over 0.54 µm). The values for the buried channel were chosen to tie in with parametric measurements of the pinning and channel potentials.

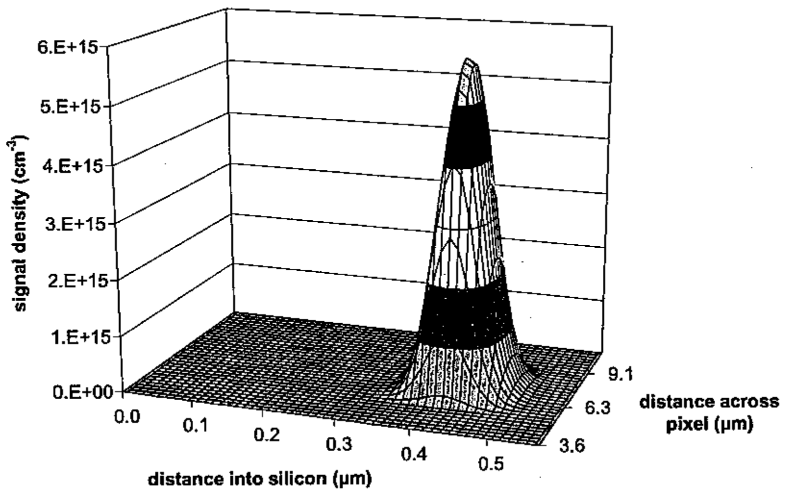

Figure 11 CCD02 2d simulation: ~9k electrons in the signal

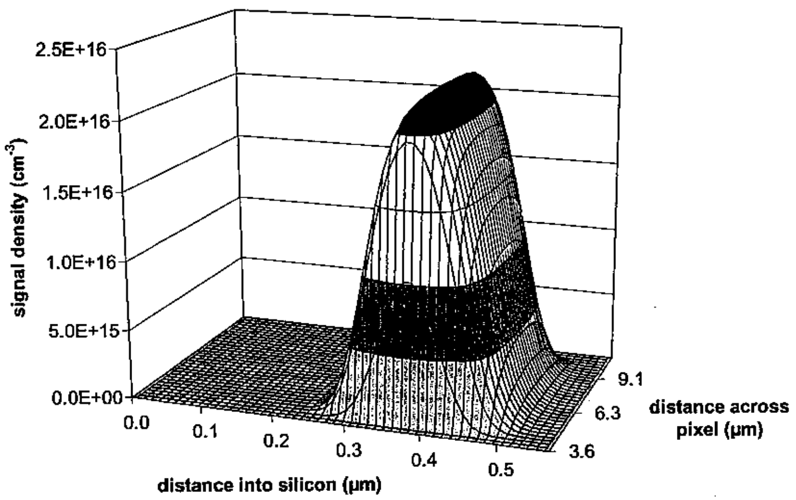

Figure 12 CCD02 2d simulation: ~270k electrons in the signal

The background signal (otherwise known as a fat zero) will effectively fill up traps within its volume. When the signal is added to the background no trapping will occur by traps filled by the background. However trapping will occur from the surrounding volume. This volume contains the low density tails of the signal distribution. As the capture time constant is inversely proportional to the signal density the capture time constant can be very long at the edges of the charge packet, thus the trapping probability can be low with a corresponding low CTI. The modelled effect of background signal on the CTI of a CCD02 device is shown in the following plot. A trap density of $1.4\ 10^{11}$ cm^{-3} was chosen as this corresponds to the estimated density of the Si-E centre after $7.2\ 10^{9}$ cm^{-2} 10 MeV equivalent protons (ionising dose of 4 krad(Si)). Here it is assumed that the traps are empty until the signal packet comes along and would be typical of what would be expected in applications running warm (i.e. around 273K).

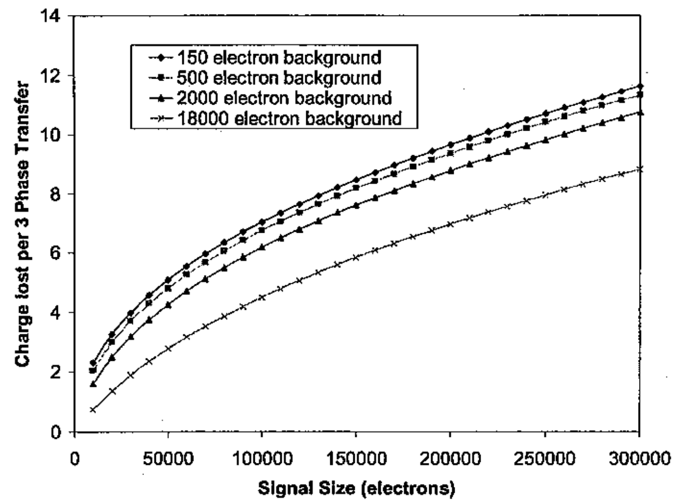

Figure 13 Results from modelling the CCD02 structure (2d simulation). The trap density was $1.4\ 10^{11}$ cm^{-3}, dwell time per phase = 0.66 µm, capture cross section = 10^{-15} cm^{2} and the emission time constant was 100 µs.

The dwell time and radiation level were chosen to compare the model with detailed measurements made by Hopkins [22] on CCD02 devices. The measured degradation was about a factor 2 higher than predicted by the model. The discrepancy may be explained by the use of a stepped doping profile in the modelling. However the modelling does show how the trapped charge is affected by the signal size and the background signal. Work is underway at Marconi to run the models with a more realistic doping profile.

This work and work performed in [22] has shown the effectiveness of background signal on reducing the CTE degradation. This reduction makes it possible to operate CCDs in a radiation environment previously thought unsuitable, for example in LEO star tracker applications.

4.5. Annealing of the CTE

If the radiation damaged silicon is heated to a sufficient temperature the radiation induced defect complexes can break apart with the constituents redistributed throughout the lattice. Measurements made by Holland [23] on proton irradiated Marconi devices showed that approximately 80% of the CTE degradation can be recovered by heating the irradiated device to 140 - 160 °C for several hours. This is consistent with the known annealing behaviour of the Si-E centre. The residual CTI is caused by the divacancy which has a much higher anneal temperature of around 330 °C. The measured half lives for 112 °C anneal was 20 hours and for 127 °C anneal was 45 hours. This is consistent with an anneal activation energy of 0.7 eV.

More detailed word performed in [8] looked the annealing of the CTI and the defect kinetics using DLTS. It is clear that the break up of the Si-E centre results in other defect complexes increasing in density, for example the Si-A centre. It was pointed out that, although annealing will initially reduce the CTI, over annealing may cause the CTI to increase, depending on the operating conditions.

5. LATCH-UP

Heavy ion testing or analysis has not been performed on Marconi devices. There does exist within the CCD a parasitic thyristor structure. This structure has been considered and it is clear that under 'normal' conditions the thyristor cannot be made to turn on. The thyristor consists of the CCD substrate, forming the gate of the thyristor, the CCD gate protected gates connected to the thyristor anode and the CCD drains connected to the thyristor cathode. The only way this structure can turn on is if the gates are at a higher potential than the drains. The condition for current flow, and therefore latch-up, is not fulfilled under normal operating conditions. Therefore, under normal operating conditions (biased or connections grounded) the device should be latch-up free.

6. CONCLUSION

This document has briefly described the main radiation effects in Marconi devices. The radiation levels that can be survived by the CCD are dependent on the performance required, the operating conditions and the device structure. The picture is a complicated one and, although much useful prediction work can be undertaken, it is recommended that, if a device is to be used in a performance critical application, evaluation be undertaken using operating conditions as close as possible to those used in the instrument. This is particularly important in the assessment of image degradation due to charge trapping.

7. REFERENCES

Note that some of these references are for limited circulation only.

[1] M Robbins, "Radiation Damage Effects in Charge Coupled Devices", Phd Thesis 1992

[2] T Roy, "Ionising Radiation Induced Surface Effects in Charge Coupled Devices", Phd Thesis 1993

[3] M Tudge "Long and Short Term Effects of X-Rays on Charge Coupled Devices", Phd Thesis 1995

[4] MERIS Phase C/D Evaluation Report, Marconi doc number PO-RP-EEV-ME-069, 1996

[5] MERIS Phase C/D FM CCD Lot Acceptance Test (LAT) Report, EEV doc number PO-RP-EEV-ME-086, 1996

[6] CCD25-20 CCD Radiation Test Report, Marconi doc number EEV-RP-012, 1999

[7] D. Herve et al, "Cumulated Dose Long Term Effects in Charge Coupled Devices", IEEE Proceedings of RADECS 91, 343-347, 1991.

[8] Watts S J, Holmes-Siedle A, Holland A "Further Radiation Evaluation of X-ray Sensitive Charge Coupled Devices for the XMM Telescope" Final Report on ESTEC Contract 8815/90/NL/LC(SC) 1995

[9] G Hopkinson "Final Report of Proton Radiation Testing of CCDs for the SILEX Programme" ESTEC contract number 7787/NL/DG 1991.

[10] C J Dale et al "The generation lifetime damage factor and its variance in silicon", IEEE Trans. Nucl. Sci, NS-36, 1872-1881 (1989)

[11] M Robbins "Proton induced dark signal distribution in CCDs" To be published.

[12] P A Martin et al "Electric field enhanced emission from non-Coulombic traps in semiconductors", J. Appl. Phys. 52, 1981, pp7409-7415

[13] G Hopkinson "Final Report on CCD Radiation Damage Study" ESTEC Contract 9557/NL/LC(SC) 1995

[14] I Hopkins, G Hopkinson "Random Telegraph Signals from Proton Irradiated CCDs" IEEE Trans Nucl Sci, Vol 40, 1993, 1567-1574

[15] D J Burt, R T Bell " Investigation of Dither Mode Clocking" Marconi Technical Document Dated 7 September 1993.

[16] K Hadfield "Practical Aspects of Dither Clocking" Marconi Technical Document Dated 23 February 1998.

[17] GOMOS Phase A/B Evaluation Report, Marconi doc number PO-RP-EEV-GM-064, 1996

[18] G J Brucker et al "The damage equivalence of electrons, protons, and gamma rays in MOS devices" IEEE Trans Nucl Sci, Vol 29, 1982 1966-1969

[19] R W Tallon et al "Radiation damage in MOS transistors as a function of the angle between applied electric field and various incident radiations (protons, electrons and Co60 gamma rays" IEEE Trans Nucl Sci, Vol 34, 1987 1208-1213

[20] G R Hopkinson, C J Dale, P W Marshall "Proton effects in charge coupled devices" IEEE Trans Nucl Sci, Vol 43, 1996, 614-627

[21] Hardy et al "Charge Transfer Efficiency in Proton Damaged CCDs" IEEE Trans Nucl Sci, Vol 45, 1998 154-163

[22] I H Hopkins, G R Hopkinson and B Johlander "Proton-Induced Charge Transfer Degradation in CCDs for Near Room Temperature Applications" IEEE Trans Nucl Sci, Vol 41, 1994, 1984-1991

[23] A D Holland "Annealing of proton-induced displacement damage in CCDs for space use" Proc 10th Symposium on Photoelectronic Image Devices, 1991, 33-40, edited by B L Morgan